

Extended Higgs sectors, vacuum stability and related issues

Nabarun Chakrabarty
National Center for Theoretical Sciences, Hsinchu, Taiwan

June 29, 2018

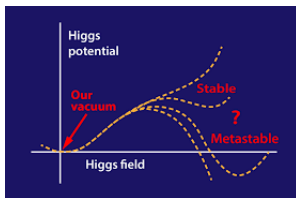
Based on works done in collaboration with Biswarup Mukhopadhyaya, Ipsita Saha, Dilip Kumar Ghosh and Ujjal Kumar Dey.

Outline

- Fate of the EW vacuum in the SM
- Two Higgs doublet models
 - (a) The Type-II 2HDM and a stable EW vacuum
 - (b) Possible collider signals
 - (c) The inert version of a 2HDM: DM, neutrino mass and vacuum stability
- 3HDM with a global S_3 symmetry
- Conclusions

A new vacuum.

- In the Standard Model (SM), there lies the possibility of having a vacuum at high energy scales, that is deeper than the electroweak (EW) vacuum.
- Arises on incorporating renormalization group (RG) effects to the couplings.



New vacuum shallower (than EW vacuum) \rightarrow *stable EW vacuum.*

New vacuum deeper and $\tau_{\text{tunnelling}} > \tau_{\text{Universe}}$ \rightarrow *metastable EW vacuum.*

New vacuum deeper and $\tau_{\text{tunnelling}} < \tau_{\text{Universe}}$ \rightarrow *unstable EW vacuum.*

Metastability criterion from vacuum tunnelling.

- The SM one-loop effective potential is expressed as,

$$V(h \gg v) = \frac{\lambda_{\text{eff}}}{4} h^4 \quad (1)$$

$\lambda_{\text{eff}} \rightarrow \lambda + \text{Radiative corrections}$

- Whenever $\lambda_{\text{eff}} < 0 \rightarrow$ metastable EW vacuum near the scale where $\beta_\lambda = 0$ (μ , say). In such a case, tunnelling probability is given by (Coleman, 1977)

$$p = T_U^4 \mu^4 e^{-\frac{8\pi^2}{3|\lambda_{\text{eff}}|}} \quad (2)$$

For metastability: $\lambda_{\text{eff}} \geq \frac{-0.065}{1 - 0.01 \ln(v/\mu)}$

For absolute stability: $\lambda_{\text{eff}} > 0$. (Strumia et al. 2001)

Why new physics?

- The stability of the EW vacuum turns out to be highly sensitive to M_t .

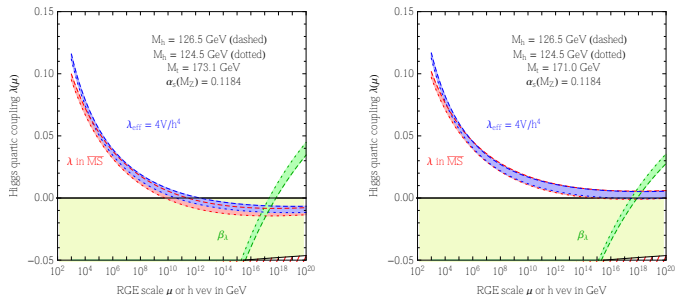


Figure: Running of λ_{eff} in the SM. Plots from paper by Elias Miro et al., 2013.

- Need more bosonic degrees of freedom to offset the fermionic drag.
- A possible choice*: Add extra scalar $SU(2)$ doublet(s) \rightarrow nHDM.

Multi-Higgs doublets.

- Multi-Higgs models open up a wonderful new world where there is the existence of charged scalars, CP violation in the scalar sector, scalar Dark Matter (DM) candidate(s), rich collider phenomenology etc.
- Additional doublets \rightarrow Additional quartic couplings \rightarrow Fast rise of such couplings \rightarrow perturbativity threatened. Moreover, possibility of enhanced Yukawa couplings that can destabilise the vacuum.
- Must there be a balance between these extremes, modulo constraints from LHC and DM experiments?
- We show our findings for two Higgs and three Higgs doublet models.

2HDM: Scalar sector

- In addition to SM fields, we add $\phi_2 \sim (1, 2, \frac{1}{2})$

$$\begin{aligned} V(\phi_1, \phi_2) = & m_{11}^2 \phi_1^\dagger \phi_1 + m_{22}^2 \phi_2^\dagger \phi_2 - m_{12}^2 (\phi_1^\dagger \phi_2 + \phi_2^\dagger \phi_1) \\ & + \frac{\lambda_1}{2} (\phi_1^\dagger \phi_1)^2 + \frac{\lambda_2}{2} (\phi_2^\dagger \phi_2)^2 \\ & + \lambda_3 \phi_1^\dagger \phi_1 \phi_2^\dagger \phi_2 + \lambda_4 \phi_1^\dagger \phi_2 \phi_2^\dagger \phi_1 + \frac{\lambda_5}{2} \left[(\phi_1^\dagger \phi_2)^2 + (\phi_2^\dagger \phi_1)^2 \right] \\ & + \lambda_6 \phi_1^\dagger \phi_1 (\phi_1^\dagger \phi_2 + \phi_2^\dagger \phi_1) + \lambda_7 \phi_2^\dagger \phi_2 (\phi_1^\dagger \phi_2 + \phi_2^\dagger \phi_1) \end{aligned}$$

- EWSB $\rightarrow \langle \phi_1 \rangle = v_1, \langle \phi_2 \rangle = v_2$
- Scalar spectrum: Charged scalar (H^\pm), CP^+ scalars (H, h), CP^- scalar (A)
- α and β mixing angles with $\tan\beta = \frac{v_2}{v_1} \rightarrow$ diagonalise the mass matrices

Model: Type II 2HDM

- Most general Yukawa interactions imply FCNCs
- Introduce \mathbb{Z}_2 symmetries

Field	\mathbb{Z}_2
$\phi_2, u_R^i, Q_L^i, L_L^i$	+
ϕ_1, d_R^i, e_R^i	-

- Couplings of h get scaled. For the Type-II case:

Coupling	Scale factor
hVV	$\sin(\beta - \alpha)$
htt	$\cos\alpha/\sin\beta$
hbb	$-\sin\alpha/\cos\beta$
htt	$-\sin\alpha/\cos\beta$

- For $\beta - \alpha = \frac{\pi}{2}$, the couplings are the corresponding SM ones \rightarrow *alignment limit* \rightarrow h signal strengths satisfied ($\mu_{\gamma\gamma}$ still needs to be checked...)

Constraints and analysis strategy

- Experimental constraints
 - (a) $m_h \sim 125$ GeV to conform with the Higgs discovery@LHC.
 - (b) $m_{H^+} > 480$ GeV to avoid flavor constraints.
 - (c) T-parameter within 0.05 ± 0.12 .
 - (d) Data on h signal strengths used.
- The theoretical constraints:
 - (a) perturbativity. ($|\lambda_i| < 4\pi$)
 - (b) unitarity.
 - (c) Vacuum stability imposed at the electroweak (EW) scale, $\mu = M_t$ (say).
($vsc1 = \lambda_1 > 0$, $vsc2 = \lambda_2 > 0$, $vsc3 = \lambda_3 + \sqrt{\lambda_1 \lambda_2} > 0$,
 $vsc4 = \lambda_3 + \lambda_4 - |\lambda_5| + \sqrt{\lambda_1 \lambda_2} > 0$)
- Parameter points clearing these constraints then allowed to evolve under Renormalisation Group (RG). Theoretical constraints imposed at each scale up to some desired cut-off → masses and mixing angles gets constrained

Main Results: Exact \mathbb{Z}_2 symmetry

- $m_{12}, \lambda_6, \lambda_7 = 0$ exact \mathbb{Z}_2 .
Any of $m_{12}, \lambda_6, \lambda_7 \neq 0 \rightarrow \mathbb{Z}_2$ breaking.
- **Exact \mathbb{Z}_2 symmetry $\rightarrow \lambda_i$ turn non-perturbative around 10 TeV.**
Parameter space of λ_i gets tight at the EW scale \rightarrow Tight bounds on the scalar masses.

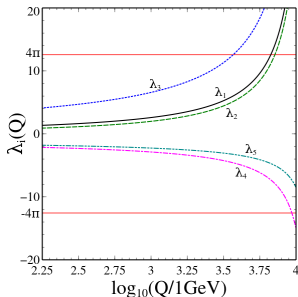
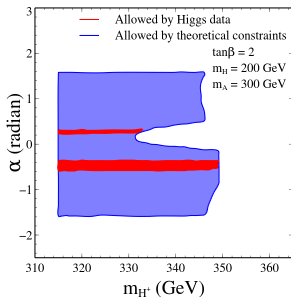


Figure: Allowed parameter spaces at $\Lambda_{UV} = 1$ TeV, $\tan\beta = 2$ and $m_{12} = 0$ GeV for $M_t = 173.1$ GeV. Running of λ_i also shown.

Main Results: \mathbb{Z}_2 breaking

- Motivates one to look beyond exact \mathbb{Z}_2 symmetry.

- We first turn on a $m_{12} \neq 0$

A benchmark: $\tan\beta = 2$, $m_{12} = 1000$ GeV, $m_h = 124.78$ GeV, $m_H = 1582.31$ GeV, $m_{H^\pm} = 1585.64$ GeV, $m_A = 1580.56$ GeV, $\alpha = 0.466$

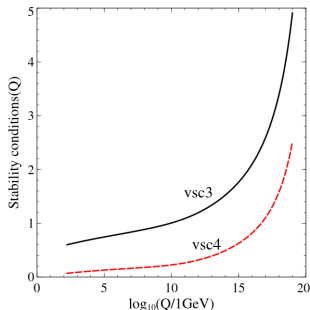
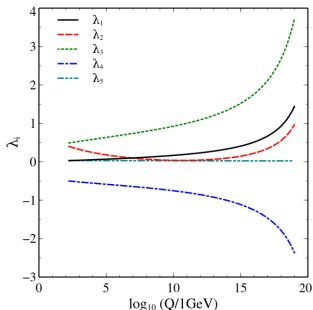


Figure: RG evolution of λ_i and the vsc's for $M_t = 173$ GeV

Main Results: \mathbb{Z}_2 breaking (soft and hard)

■ Inclusion of \mathbb{Z}_2 violating terms



EW vacuum stable till M_{Pl}

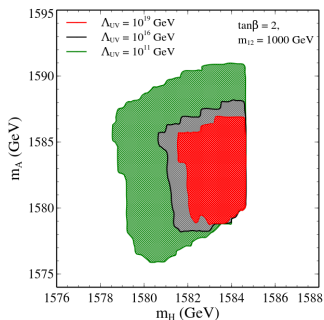
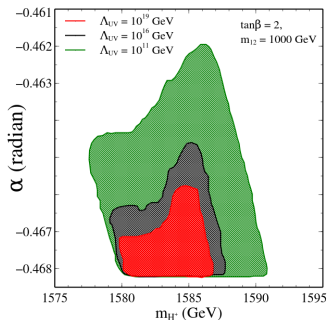


Figure: Parameter space allowing for stable vacuum till a given Λ_{UV} .

■ Parameter space gets modified, but does not disappear even for a higher M_t

Results: Features of the allowed parameter space

- The conclusions are qualitatively same for $\lambda_{6,7} \neq 0$.
- (a) Splitting among m_H , m_A and m_{H^+} is narrow.
(b) Tight constraint on $\cos(\beta - \alpha)$
- Higher is the UV cutoff, tighter are the constraints.
- Stability till $M_{Pl} \rightarrow |\cos(\beta - \alpha)| < 0.065$
for m_H , m_A and $m_{H^+} \simeq 500$ GeV
- Higher masses of the non-standard scalars \rightarrow Constraint on $\cos(\beta - \alpha)$ gets tighter

Observing at the LHC: Possible signals

- We aim to probe at the LHC a 2HDM offering a stable vacuum + perturbativity up to high energy scales.
- The following LHC signals are considered
 - (i) $pp \rightarrow H \rightarrow ZZ \rightarrow l^+l^-l^+l^-$
 - (ii) $pp \rightarrow A \rightarrow hZ \rightarrow l^+l^-bb$
- The HVV and AhZ couplings scale as $\cos(\beta - \alpha)$ in a 2HDM.
- Tight bounds on $\cos(\beta - \alpha) \rightarrow$ Observation at collider(s) can turn challenging!
- **Tools used:**
 - FeynRules \rightarrow Model implementation and generation of UFO,
 - MG5 \rightarrow MC event generation,
 - Delphes 3.2 \rightarrow Detector simulation and event analysis.

Simulation details: $pp \rightarrow H \rightarrow ZZ \rightarrow l^+l^-l^+l^-$

The following benchmark is chosen:

$m_H(\text{GeV})$	$m_A(\text{GeV})$	$m_{12}(\text{GeV})$
500	501	280

Dominant background(s):

- $pp \rightarrow ZZ(*) \rightarrow 4l$
- $pp \rightarrow Z\gamma \rightarrow 4l$

Trigger cuts (used for both the signals):

- $p_T^l \geq 10 \text{ GeV}$, $p_T^b \geq 20 \text{ GeV}$, $|\eta^{l,b}| \leq 2.5$, $\Delta R_{ll} > 0.3$, $\Delta R_{lb} > 0.4$,
 $\Delta R_{bb} > 0.4$.

Selection cuts:

- $|m_{4l} - m_H| \leq 15 \text{ GeV}$,
- $p_T^{l1} > 80 \text{ GeV}$, $p_T^{l2} > 50 \text{ GeV}$, $p_T^{l3} > 30 \text{ GeV}$, $p_T^{l4} > 20 \text{ GeV}$.
- $p_T^Z > 40 \text{ GeV}$.

Simulation details: $pp \longrightarrow A \longrightarrow hZ \longrightarrow l^+l^-bb$

Dominant background(s):

- $pp \longrightarrow t\bar{t} \longrightarrow llbb + \text{MET}$
- $pp \longrightarrow Zbb \longrightarrow llbb$
- $pp \longrightarrow ZWW \longrightarrow llbb + \text{MET}$

Selection cuts:

- $85.0 \text{ GeV} \leq m_{ll} \leq 100 \text{ GeV}$.
- $95.0 \text{ GeV} \leq m_{bb} \leq 155 \text{ GeV}$.
- $\sum_{l,b} p_T > 350 \text{ GeV}$.
- $\text{MET} \leq 30 \text{ GeV}$.
- $|m_{llbb} - m_A| \leq 30 \text{ GeV}$.
- $p_T^Z > 100 \text{ GeV}$
- $p_T^{b_1} > 50 \text{ GeV}$.

Comparing the signal significances

For fixed m_H, m_A , we show the allowed parameter space in the $\tan\beta$ vs. $\cos(\beta - \alpha)$ plane; and also the 3σ and 5σ contours for $\int \mathcal{L} dt = 3000 \text{ fb}^{-1}$.

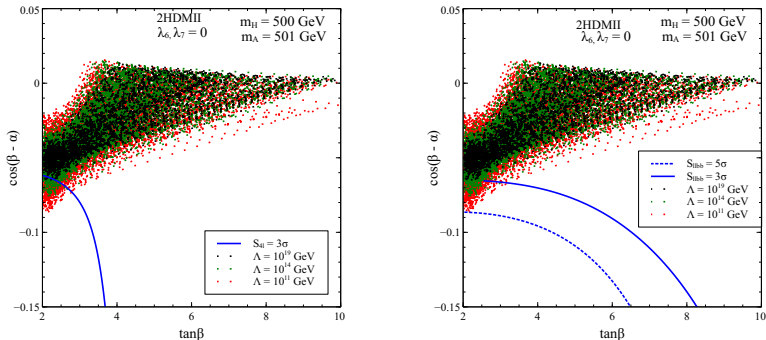


Figure: Allowed parameter space and 3σ and 5σ contours

Statistical significances of 500 GeV scalars could be at most 3σ and 5σ in the $4l$ and $l\bar{l}b\bar{b}$ channels, for the model to be valid till M_{Pl} .

Observing at the LHC: Closing remarks

- The signal $pp \rightarrow A \rightarrow hZ \rightarrow l^+l^-bb$ offers higher sensitivity.
- For $m_H, m_A \geq 550$ GeV, validity up to 10^{19} GeV yields a significance $< 3\sigma$.
- The future e^+e^- collider does not offer higher sensitivity for such heavy scalars.
This is due to the (a) Production of H is controlled by $\cos(\beta - \alpha)$
(b) For $m_H \geq 500$ GeV, $\sqrt{s} = 1$ TeV leads to kinematical limitations.
- Radiative return in a future $\mu^+\mu^-$ machine leads to enhanced observability.

A 2HDM for DM and ν -mass

- Comprises 2HDM + 3 right-handed neutrinos N_i .
- A \mathbb{Z}_2 symmetry: under which, $\Phi_2 \rightarrow -\Phi_2$ and $N_i \rightarrow -N_i$. while all other SM fields are even. Φ_2 does not receive a VEV.
- The relevant Yukawa and mass terms are

$$-\mathcal{L}_Y = (y_{ij} \bar{N}_i \tilde{\Phi}_2^\dagger \ell_j + h.c.) + \frac{M_i}{2} (\bar{N}_i^c N_i + h.c.), (i, j = 1, 2, 3) \quad (3)$$

- Mass of the active neutrinos generated at one-loop (Ma, 2006).

$$\mathcal{M}_{ij}^\nu = \sum_{k=1}^3 \frac{y_{ik} y_{jk} M_k}{16\pi^2} \left[\frac{M_H^2}{M_H^2 - M_k^2} \ln \frac{M_H^2}{M_k^2} - \frac{M_A^2}{M_A^2 - M_k^2} \ln \frac{M_A^2}{M_k^2} \right] \quad (4)$$

The neutrino masses and mixings are determined in terms of Yukawa couplings y_{ij} , inert scalar masses (M_H, M_A) and three heavy neutrino masses $M_{1,2,3}$.

A 2HDM for DM and ν -mass

- **Assumptions:** (a) M_1 is mass of the lightest state and considered two values, namely, $M_1 = M = 110$ TeV and 10^9 TeV.
(b) Only one dominant diagonal Yukawa coupling, y_ν (say). Leptogenesis puts a lower bound on M , (Pilaftsis, 1997, Hambye 2009)
- y_ν determined by demanding $M_\nu \sim 0.1$ eV.
- *Introduction of $N_i \rightarrow$ Additional terms in the IDM beta functions.*

$$16\pi^2 \frac{d\lambda_2}{dt} \Big|_{IDM+RH} = 16\pi^2 \frac{d\lambda_2}{dt} \Big|_{IDM} + 4\lambda_2 y_\nu^2 - 4y_\nu^4,$$

$$16\pi^2 \frac{d\lambda_i}{dt} \Big|_{IDM+RH} = 16\pi^2 \frac{d\lambda_i}{dt} \Big|_{IDM} + 4\lambda_i y_\nu^2, \quad (i = 3, 4, 5),$$

$$16\pi^2 \frac{dy_\nu}{dt} \Big|_{IDM+RH} = y_\nu \left(-\frac{9}{4}g^2 - \frac{3}{4}g'^2 + \frac{5}{2}y_\nu^2 \right).$$

- Evolution from the weak scale till M using the purely IDM RGEs. We incorporate the effect of N_i for energy scales above the M threshold.
- $M = 110$ TeV $\rightarrow y_\nu = O(10^{-4}) \rightarrow$ *No impact on RG evolution.*
 $M = 10^9$ TeV $\rightarrow y_\nu = O(0.1) \rightarrow$ *Noticable impact on RG evolution.*

DM phenomenology in a nutshell.

- H or A could be viable DM candidates. We arrange for $M_H < M_A$ and hence take H to be the DM candidate. $\Omega h^2 \simeq 0.1$ is obtained in the following two regions:
- $H - H - h$ interaction strength $\longrightarrow -\lambda_L v = -(\lambda_3 + \lambda_4 + \lambda_5)v$.
- $50 \text{ GeV} \leq M_H \leq M_W \text{ GeV}$: Ωh^2 mainly generated by s-channel DM annihilation through h exchange (Arhrib et. al. JHEP 2013). For $M_H > M_W \text{ GeV}$, $\langle \sigma v \rangle$ increases due to kinematic access to the VV final state thereby bringing down the relic.
- $M_H \geq 500 \text{ GeV}$: Cancellation occurs between the $H - H - V - V$ vertex driven diagrams, and the t/u-channel diagrams whenever $m_H \simeq m_A \simeq m_{H^+}$. A part of the relic then generated from co-annihilations
- DM-nucleon cross section generated through t-channel h exchange

Main results: $M_H < M_W$

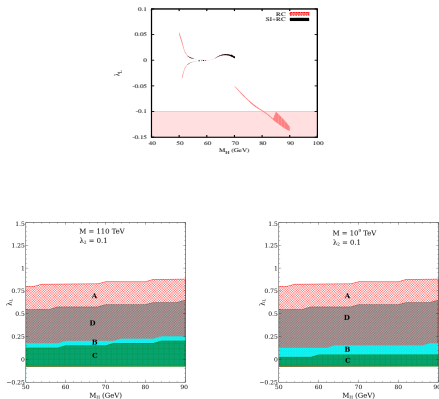


Figure: Region(s) allowed in the $M_H - \lambda_L$ plane obeying the DM constraints (top) and RG constraints for $M = 110 \text{ TeV}$ (bottom left) and $M = 10^9 \text{ TeV}$ (bottom right). The overlapped regions labelled by **A** (red), **B** (cyan) and **C** (green) are consistent with the theoretical constraints up to $\Lambda_{UV} = 10^6, 10^{16}$ and 10^{19} GeV respectively.

Main results: $M_H < M_W$

We find...

- **Sizable parameter space exists obeying the DM constraints and also theoretical constraints upto the Planck scale.**
- **Upper bounds on M_H^\pm and M_A are obtained at $\simeq 150\text{-}170$ GeV by requiring perturbative unitarity till M_{Pl} .**
- $\lambda_3 + \sqrt{\lambda_1 \lambda_2} \geq 0$ forbids large negative values of λ_3 and perturbativity puts an upper bound \rightarrow similar bound on λ_L .
- The fact that λ_3 can not be large negative results in decrease in the $h \rightarrow \gamma\gamma$ signal strength.
- The allowed parameter space shrinks by switching over from $M = 110$ TeV to $M = 10^9$ TeV (albeit not greatly).

Results: $M_H > 500$ GeV

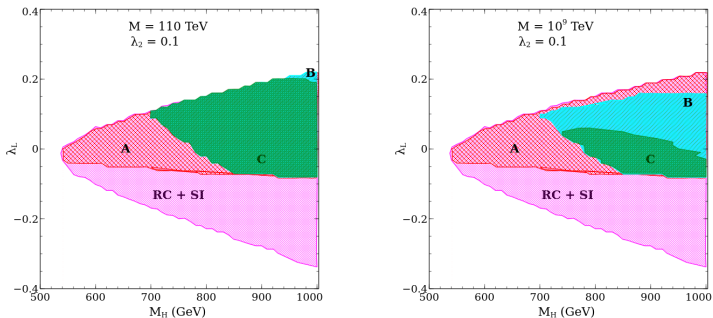


Figure: Region(s) allowed in the M_H - λ_L plane obeying the various constraints for $M = 110$ TeV (left panel) and $M = 10^9$ TeV (right panel). The full region (marked by 'RC + SI') (magenta) is allowed by the DM constraints alone. The overlapped regions labelled by **A** (red), **B** (cyan) and **C** (green) are consistent with the theoretical constraints up to $\Lambda_{UV} = 10^6, 10^{16}$ and 10^{19} GeV respectively.

Results: $M_H > 500$ GeV

- Vacuum stability till $M_{Pl} \rightarrow M_H > 700$ GeV.
- **The parameter space valid till M_{Pl} shrinks significantly upon switching from $M = 110$ TeV to $M = 10^9$ TeV.** A stronger bound $M_H > 740$ GeV obtained for the latter.
- **Reason:** Whenever $M_H \simeq M_A$ and $M = 10^9$ TeV, y_ν becomes $\mathcal{O}(0.1)$. Such a large Yukawa coupling contributes to the beta function of λ_2 through the terms $+\lambda_2 y_\nu^2$ and $-y_\nu^4$ that either makes λ_2 non-perturbative in some cases or λ_2 negative in the other and subsequently the vacuum unstable.

Results: $M_H > 500$ GeV regime

BP	M_H	M_{H^\pm}	M_A	λ_L	λ_2
BP2	710.0 GeV	712.0 GeV	711.0 GeV	0.11	0.1

Table: Benchmark values (BP) of parameters affecting the RG evolution of the quartic couplings. For each BP, two values of M , namely, 110 TeV and 10^9 TeV, have been used.

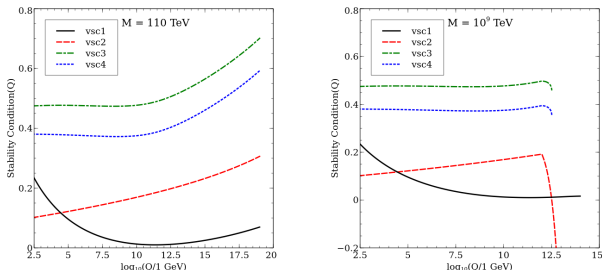


Figure: RG running of different scalar quartic couplings corresponding to BP2. The solid, dashed, dashed dotted and dotted lines denote the evolution curves of the stability conditions vsc1, vsc2, vsc3 and vsc4 respectively.

Overall remarks on the 2HDM results.

- A 2HDM indeed can stabilise the EW vacuum up to as high as the Planck scale.
- This does not come into conflict with *low energy* experimental data such as those on signal strengths, flavour observables and oblique parameters.
- Probing such a model at the LHC could turn challenging!
- A light ν -mass, correct thermal relic and right leptogenesis parameters are obtainable from the *inert* case of the 2HDM framework. The same parameter space allows for vacuum stability till the Planck scale.
- We need not break the \mathbb{Z}_2 symmetry explicitly for stability till high scales. Changing the EWSB pattern can serve the purpose!

An S_3 symmetric 3HDM

- What could be the result of such investigations for a 3HDM?
(Proposed by Weinberg to study spontaneous CP violation (PRL, 1976).)
- A large number of parameters, wide scalar spectrum: 2 charged scalars (H_1^+ , H_2^+), 2 CP^- scalars (A_1 , A_2) and 3 CP^+ scalars (h , H_1 , H_2) → **Difficult to handle!**
- **Possible way out?** → Introduce symmetries to reduce the number of parameters
- Various discrete non-Abelian symmetries (A_4 , S_4 , S_3 ...) can be imposed → Can reproduce fermion spectrum and the mixings
- Results demonstrated in case of the discrete symmetry S_3

S_3 HDM: Scalar sector

- S_3 symmetry: ϕ_1 and ϕ_2 transform as doublets, ϕ_3 as a singlet.
The elements of S_3 for this particular doublet representation, :

$$\begin{pmatrix} \cos \theta & \sin \theta \\ -\sin \theta & \cos \theta \end{pmatrix}, \quad \begin{pmatrix} \cos \theta & \sin \theta \\ \sin \theta & -\cos \theta \end{pmatrix}, \quad \text{for } \left(\theta = 0, \pm \frac{2\pi}{3} \right). \quad (5)$$

$$\begin{aligned} V(\phi) = & \mu_{11}^2(\phi_1^\dagger\phi_1 + \phi_2^\dagger\phi_2) + \mu_{33}^2\phi_3^\dagger\phi_3 \\ & + \lambda_1(\phi_1^\dagger\phi_1 + \phi_2^\dagger\phi_2)^2 + \lambda_2(\phi_1^\dagger\phi_2 - \phi_2^\dagger\phi_1)^2 \\ & + \lambda_3 \left\{ (\phi_1^\dagger\phi_2 + \phi_2^\dagger\phi_1)^2 + (\phi_1^\dagger\phi_1 - \phi_2^\dagger\phi_2)^2 \right\} \\ & + \lambda_4 \left\{ (\phi_3^\dagger\phi_1)(\phi_1^\dagger\phi_2 + \phi_2^\dagger\phi_1) + (\phi_3^\dagger\phi_2)(\phi_1^\dagger\phi_1 - \phi_2^\dagger\phi_2) + \text{h.c.} \right\} \\ & + \lambda_5(\phi_3^\dagger\phi_3)(\phi_1^\dagger\phi_1 + \phi_2^\dagger\phi_2) + \lambda_6 \left\{ (\phi_3^\dagger\phi_1)(\phi_1^\dagger\phi_3) + (\phi_3^\dagger\phi_2)(\phi_2^\dagger\phi_3) \right\} \\ & + \lambda_7 \left\{ (\phi_3^\dagger\phi_1)(\phi_3^\dagger\phi_1) + (\phi_3^\dagger\phi_2)(\phi_3^\dagger\phi_2) + \text{h.c.} \right\} + \lambda_8(\phi_3^\dagger\phi_3)^2. \quad (6a) \end{aligned}$$

S_3 HDM: Scalar sector

- μ_{11} and μ_{33} can be traded by the tadpole equations. For consistency of the tadpole relations, the following are the possibilities:

$$v_1 = \sqrt{3}v_2, \quad (7a)$$

$$\text{or, } v_1 = v_2 = 0, v_3 = 246 \text{ GeV}, \quad (7b)$$

$$\text{or, } \lambda_4 = 0 \text{ and } v_1, v_2, v_3 \text{ independent.} \quad (7c)$$

- (c) leads to a massless physical scalar \rightarrow *disfavoured by meson mixing data*
- For (a), we introduce $\tan\beta = \frac{2v_2}{v_3}$ and α as the mixing angles
- For $\beta - \alpha \simeq \frac{\pi}{2}$, the couplings of h are SM-like \rightarrow an *alignment* limit like in the 2HDM
- Cases (a) and (b) considered for subsequent analyses

S_3 HDM: Yukawa sector

- Multiple patterns of SSB possible!
(a) All three doublets get VEV $\rightarrow \langle \phi_1 \rangle = v_1, \langle \phi_2 \rangle = v_2, \langle \phi_3 \rangle = v_3$
 \rightarrow active scenario
- In the u -quark sector: (Q_{1L}, Q_{2L}) and (u_{1R}, u_{2R}) are S_3 doublets.
 $Q_{3L}, u_{3R} \rightarrow S_3$ singlets

$$\begin{aligned} -\mathcal{L}_Y^u &= y_1^u \left(\bar{Q}_1 \tilde{\phi}_3 u_{1R} + \bar{Q}_2 \tilde{\phi}_3 u_{2R} \right) \\ &+ y_2^u \left\{ \left(\bar{Q}_1 \tilde{\phi}_2 + \bar{Q}_2 \tilde{\phi}_1 \right) u_{1R} + \left(\bar{Q}_1 \tilde{\phi}_1 + \bar{Q}_2 \tilde{\phi}_2 \right) u_{2R} \right\} \\ &+ y_3^u \bar{Q}_3 \tilde{\phi}_3 u_{3R} + y_4^u \bar{Q}_3 \left(\tilde{\phi}_1 u_{1R} + \tilde{\phi}_2 u_{2R} \right) + y_5^u \left(\bar{Q}_1 \tilde{\phi}_1 + \bar{Q}_2 \tilde{\phi}_2 \right) u_{3R} + \text{h.c.} \end{aligned}$$

- Can explain the quark sector mass hierarchy, flavor mixing V_{CKM} and measure of CP violation naturally. (see [Teshima 2005](#))

S_3 HDM: Scalar sector

- **(b) Two doublets remain inert** $\rightarrow \langle \phi_{1,2} \rangle = 0, \langle \phi_3 \rangle = v$
- All fermions are S_3 singlets in this case

$$-\mathcal{L}_Y^u = y_1^u \bar{Q}_1 \tilde{\phi}_3 u_{1R} + y_2^u \bar{Q}_2 \tilde{\phi}_3 u_{2R} + y_3^u \bar{Q}_3 \tilde{\phi}_3 u_{3R} + \text{h.c.}$$

- $\lambda_4 = 0 \rightarrow$ Unbroken $Z_2 \rightarrow$ degenerate mass spectrum:

$$\begin{aligned} m_{H_1}^2 &= m_{H_2}^2 = \mu_{11}^2 + \frac{1}{2}(\lambda_5 + \lambda_6 + 2\lambda_7)v^2 \\ m_{A_1}^2 &= m_{A_2}^2 = \mu_{11}^2 + \frac{1}{2}(\lambda_5 + \lambda_6 - 2\lambda_7)v^2 \\ m_{H_1^+}^2 &= m_{H_2^+}^2 = \mu_{11}^2 + \frac{1}{2}\lambda_5 v^2 \end{aligned}$$

- Interesting from the perspective of DM
- H_1 and H_2 can be DM candidates $\rightarrow \Omega h^2 = \Omega_{H_1} h^2 + \Omega_{H_2} h^2$.

$S_3 \times Z_2$ HDM: Vacuum stability and related issues

- **Theoretical constraints:** (a) Perturbativity. ($|\lambda_i| < 4\pi$)
(b) Unitarity. ($|a_i| < 8\pi$)
(c) Bounded from below:

$$\text{vsc1} : \lambda_1 > 0, \quad (8)$$

$$\text{vsc2} : \lambda_8 > 0, \quad (9)$$

$$\text{vsc3} : \lambda_1 + \lambda_3 > 0, \quad (10)$$

$$\text{vsc4} : 2\lambda_1 + (\lambda_3 - \lambda_2) > |\lambda_2 + \lambda_3|, \quad (11)$$

$$\text{vsc5} : \lambda_5 + 2\sqrt{\lambda_8(\lambda_1 + \lambda_3)} > 0, \quad (12)$$

$$\text{vsc6} : \lambda_5 + \lambda_6 + 2\sqrt{\lambda_8(\lambda_1 + \lambda_3)} > 2|\lambda_7|, \quad (13)$$

$$\text{vsc7} : \lambda_1 + \lambda_3 + \lambda_5 + \lambda_6 + 2\lambda_7 + \lambda_8 > 2|\lambda_4|. \quad (14)$$

$S_3 \times Z_2$ HDM: Vacuum stability and related issues

- **Experimental constraints:** (a) $m_h = 125$ GeV, $m_{H_i^+}, m_{A_i} > 100$ GeV. (b) S, T and U parameters within their allowed bands (c) Dark matter relic and SI-cross section.
- One loop RGEs derived using scale invariance of the 1-loop effective potential. *Consistency check:* Feynman diagrammatic calculation.
An Example,

$$16\pi^2\beta_{\lambda_8} = 4\lambda_5^2 + 4\lambda_5\lambda_6 + 2\lambda_6^2 + 8\lambda_7^2 + 24\lambda_8^2 + \frac{3}{8}(g'^4 + 2g'^2g^2 + 3g^4) - \lambda_8(9g^2 + 3g'^2 - 12(y_3^u)^2) - 6(y_3^u)^4,$$

(See PRD 93, 075025 (2016) for a complete list)

Main results: Active scenario

- The active scenario not valid beyond $\sim 10^7$ GeV

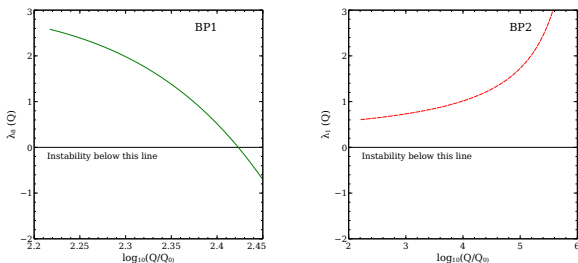


Figure: RG running of different scalar quartic couplings corresponding to two different benchmarks. We use $M_t = 173$ GeV for the entire analysis.

- *Underlying reason(s)*

(a) In absence of dimensionful parameters, $\lambda_i \sim \frac{m^2}{v^2}$. Large values to λ_i at the input scale \rightarrow Non perturbative behaviour soon after.

(b) High $\tan\beta \rightarrow$ Enhanced fermionic downward pull on λ_8 . \rightarrow Destabilised vacuum.

Main results: Inert scenario

- $\Omega h^2 \sim 0.1$ achieved for $m_{H_1} < 80 \text{ GeV} \cup m_{H_1} > 370 \text{ GeV}$. (As opposed to $m_H < 80 \text{ GeV} \cup m_H > 500 \text{ GeV}$ for a single inert doublet.)

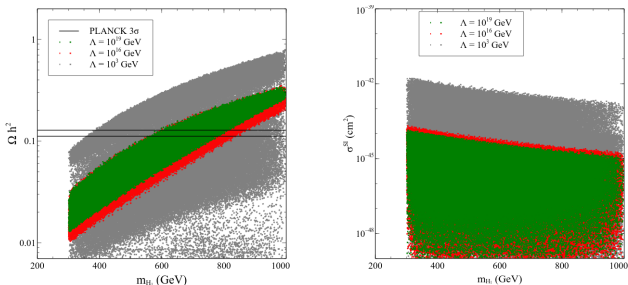


Figure: Prediction of Ωh^2 and SI cross section for model points valid till various cut-off scales. Colour coding to be read from the legends.

- **Stable EW vacuum + perturbative unitarity till $M_{Pl} \rightarrow$**
 $\Omega h^2 \sim 0.1$ achieved for $m_{H_1} < 80 \text{ GeV} \cup m_{H_1} > 570 \text{ GeV}$

Main results: Inert scenario

$$\lambda_5 = \lambda_L + \frac{2}{v^2}(m_{H_1^+}^2 - m_{H_1}^2)$$

$$\lambda_6 = \frac{1}{v^2}(m_{H_1}^2 + m_{A_1}^2 - 2m_{H_1^+}^2)$$

$$\lambda_7 = \frac{1}{2v^2}(m_{H_1}^2 - m_{A_1}^2)$$

■ *Underlying reasons*

(a) When $m_{H_1} < 80$ GeV, $m_{A_1}, m_{H_1^+}$ can be chosen freely so as to give the right values to $\lambda_5, \lambda_6, \lambda_7$ such that vacuum stability till M_{Pl} is ensured.

(b) Very heavy $m_{A_1}, m_{H_1^+} \rightarrow \lambda_5, \lambda_6, \lambda_7$ become large at the EW scale \rightarrow Non-perturbative behaviour!

(c) Thus, $m_{A_1}, m_{H_1^+} < 135$ GeV for a perturbative model till M_{Pl} .

Main results: Inert scenario

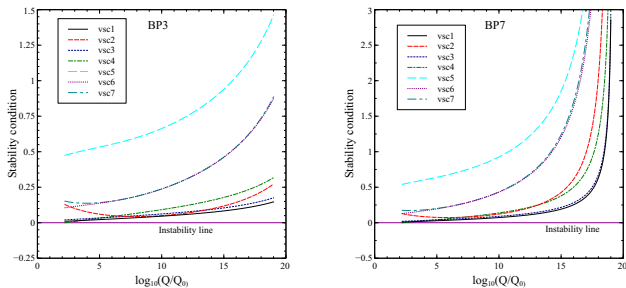


Figure: Prediction of Ωh^2 and SI cross section for model points valid till various cut-off scales. Colour coding to be read from the legends.

(e) When $m_{H_1} > 370$ GeV, $m_{A_1}, m_{H_1^+} \simeq m_{H_1}$. Appropriate choice of $m_{H_1} \longrightarrow$ Proper values to $\lambda_5, \lambda_6, \lambda_7$

(f) Therefore, a vacuum stability till M_{Pl} plus correct relic demands $m_{H_1} > 570$ GeV.

Conclusions.

- Multi-Higgs scenarios could gain more importance in the future. Two- and Three- Higgs doublet scenarios can indeed alleviate the vacuum instability problem faced by the SM.
- The conclusions regarding high-scale validity depend on the presence (or absence!) of global symmetries, as well as the EWSB pattern.
- High-scale stability can comply with various experimental observations such as that of DM and neutrino mass.
- Discovery of additional scalars at the upcoming collisions awaited. That must be followed up by a precise measurement of their couplings to the SM fields. The fate of the EW vacuum is then sealed.
- *Possible future directions:* Incorporating finite temperature effects and studying vacuum (meta)stability in the scenarios just discussed.

References for this talk

- High-scale validity of a two Higgs doublet scenario: predicting collider signals
Nabarun Chakrabarty and Biswarup Mukhopadhyaya,
Phys. Rev. D 96, 035028
- High-scale validity of a model with Three-Higgs-doublets
Nabarun Chakrabarty, Phys. Rev. D 93, 075025 (2016)
- Dark matter, neutrino masses and high scale validity of an inert Higgs doublet model
Nabarun Chakrabarty, Dilip Kumar Ghosh, Biswarup Mukhopadhyaya, Ipsita Saha, Phys. Rev. D 92, 015002 (2015).
- High-scale validity of a two-Higgs doublet scenario: a study including LHC data
Nabarun Chakrabarty, Ujjal Kumar Dey, Biswarup Mukhopadhyaya,
JHEP12(2014)166.

*Thank you
for your attention*

Back up slides...

Possibility of a metastable EW vacuum

- The t -quark Yukawa is enhanced *w.r.t* the SM (scales by $\frac{\cos\alpha}{\sin\beta}$). The t -quark couples to ϕ_2 in Type-II 2HDM. $\rightarrow \lambda_2$ **can turn negative while evolution**.
- Assumption: Metastable EW vacuum occurs in the ϕ_2 direction, we use the following condition to identify it,

$$0 \geq \lambda_2^{eff} \geq \frac{-0.065}{1 - 0.01 \ln(v/\mu)} \quad (15)$$

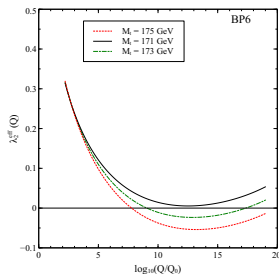


Figure: Running of λ_2 for different M_t . We have $\tan\beta=10.94$, $m_h=125$ GeV, $m_H=1499$ GeV, $m_A=1500$ GeV, $m_{H^\pm}=1498$ GeV, $\beta - \alpha = \frac{\pi}{2}$

Possibility of a metastable EW vacuum

- Low $\tan\beta \rightarrow$ Vacuum tends to turn metastable.
- The bound on $\tan\beta$ sensitive to the value of M_t chosen.

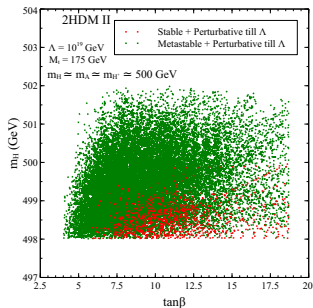
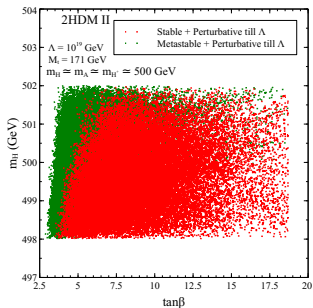


Figure: Figure describing the lower bounds on $\tan\beta$ from the requirement of stability and metastability, for the non-standard masses around 500 GeV.

- In all, TypeII 2HDM certainly fares better than the SM from the vacuum stability perspective. Should be true for other 2HDMs too.

One-loop beta functions

The RG equations for the gauge couplings, for this model, are given by [?],

$$16\pi^2 \frac{dg_s}{dt} = -7g_s^3,$$

$$16\pi^2 \frac{dg}{dt} = -3g^3,$$

$$16\pi^2 \frac{dg'}{dt} = 7g'^3.$$

Here g' , g and g_s denote the $U(1)$, $SU(2)_L$ and $SU(3)_c$ gauge couplings respectively.

One-loop beta functions

$$16\pi^2 \frac{d\lambda_1}{dt} = 12\lambda_1^2 + 4\lambda_3^2 + 4\lambda_3\lambda_4 + 2\lambda_4^2 + 2\lambda_5^2 + \frac{3}{4}(3g^4 + g'^4 + 2g^2g'^2) - \lambda_1(9g^2 + 3g'^2 - 12y_t^2 - 12y_b^2 - 4y_\tau^2) - 12y_t^4,$$

$$16\pi^2 \frac{d\lambda_2}{dt} = 12\lambda_2^2 + 4\lambda_3^2 + 4\lambda_3\lambda_4 + 2\lambda_4^2 + 2\lambda_5^2 + \frac{3}{4}(3g^4 + g'^4 + 2g^2g'^2) - 3\lambda_2(3g^2 + g'^2 - \frac{4}{3}y_\nu^2) - 4y_\nu^4,$$

$$16\pi^2 \frac{d\lambda_3}{dt} = (\lambda_1 + \lambda_2)(6\lambda_3 + 2\lambda_4) + 4\lambda_3^2 + 2\lambda_4^2 + 2\lambda_5^2 + \frac{3}{4}(3g^4 + g'^4 - 2g^2g'^2) - \lambda_3(9g^2 + 3g'^2 - 6y_t^2 - 6y_b^2 - 2y_\tau^2 - 2y_\nu^2),$$

$$16\pi^2 \frac{d\lambda_4}{dt} = 2(\lambda_1 + \lambda_2)\lambda_4 + 8\lambda_3\lambda_4 + 4\lambda_4^2 + 8\lambda_5^2 + 3g^2g'^2 - \lambda_4(9g^2 + 3g'^2 - 6y_t^2 - 6y_b^2 - 2y_\tau^2 - 2y_\nu^2),$$

$$16\pi^2 \frac{d\lambda_5}{dt} = (2\lambda_1 + 2\lambda_2 + 8\lambda_3 + 12\lambda_4)\lambda_5 - \lambda_5(9g^2 + 3g'^2 - 6y_b^2 - 2y_\tau^2 - 6y_t^2 -$$

$$\begin{aligned}
16\pi^2 \frac{dy_b}{dt} &= y_b \left(-8g_s^2 - \frac{9}{4}g^2 - \frac{5}{12}g'^2 + \frac{9}{2}y_b^2 + y_\tau^2 + \frac{3}{2}y_t^2 \right), \\
16\pi^2 \frac{dy_t}{dt} &= y_t \left(-8g_s^2 - \frac{9}{4}g^2 - \frac{17}{12}g'^2 + \frac{9}{2}y_t^2 + y_\tau^2 + \frac{3}{2}y_b^2 \right), \\
16\pi^2 \frac{dy_\tau}{dt} &= y_\tau \left(-\frac{9}{4}g^2 - \frac{15}{4}g'^2 + 3y_b^2 + 3y_t^2 + \frac{1}{2}y_\nu^2 + \frac{5}{2}y_\tau^2 \right), \\
16\pi^2 \frac{dy_\nu}{dt} &= y_\tau \left(-\frac{9}{4}g^2 - \frac{3}{4}g'^2 - \frac{3}{4}y_\tau^2 + \frac{5}{2}y_\nu^2 \right).
\end{aligned}$$

Lee-Quigg-Thacker eigenvalues.

$$a_{\pm} = \frac{3}{2}(\lambda_1 + \lambda_2) \pm \sqrt{\frac{9}{4}(\lambda_1 - \lambda_2)^2 + (2\lambda_3 + \lambda_4)^2},$$

$$b_{\pm} = \frac{1}{2}(\lambda_1 + \lambda_2) \pm \sqrt{\frac{1}{4}(\lambda_1 - \lambda_2)^2 + \lambda_4^2},$$

$$c_{\pm} = d_{\pm} = \frac{1}{2}(\lambda_1 + \lambda_2) \pm \sqrt{\frac{1}{4}(\lambda_1 - \lambda_2)^2 + \lambda_5^2},$$

$$e_1 = (\lambda_3 + 2\lambda_4 - 3\lambda_5),$$

$$e_2 = (\lambda_3 - \lambda_5),$$

$$f_1 = f_2 = (\lambda_3 + \lambda_4),$$

$$f_+ = (\lambda_3 + 2\lambda_4 + 3\lambda_5),$$

$$f_- = (\lambda_3 + \lambda_5),$$

$$p = (\lambda_3 - \lambda_4).$$

Constraints: Collider

Channel	Experiment	$\hat{\mu}$	Energy in TeV (Luminosity in fb^{-1})
$h \rightarrow \gamma\gamma$	ATLAS	$1.55^{+0.33}_{-0.28}$	7 (4.8) + 8 (20.7)
	CMS	$0.78^{+0.28}_{-0.26}$	7 (5.1) + 8 (19.6)
$h \xrightarrow{ZZ^*} 4l$	ATLAS	$1.43^{+0.40}_{-0.35}$	7 (4.6) + 8 (20.7)
	CMS	$0.93^{+0.29}_{-0.25}$	7 (5.1) + 8 (19.7)
$h \xrightarrow{WW^*} 2l2\nu$	ATLAS	$0.99^{+0.31}_{-0.28}$	7 (4.6) + 8 (20.7)
	CMS	$0.72^{+0.20}_{-0.18}$	7 (4.9) + 8 (19.4)
$h \rightarrow b\bar{b}$	ATLAS	$0.20^{+0.70}_{-0.60}$	7 (4.7) + 8 (20.3)
	CMS	$1.00^{+0.50}_{-0.50}$	7 (5.1) + 8 (18.9)
$h \rightarrow \tau\bar{\tau}$	ATLAS	$1.4^{+0.50}_{-0.40}$	8 (20.3)
	CMS	$0.78^{+0.27}_{-0.27}$	7 (4.9) + 8 (19.7)

Table: The signal strengths in various channels with their 1σ uncertainties.

Muon collider results

Benchmark	\sqrt{s} (GeV)	$\tan\beta$	m_H (GeV)	m_A (GeV)
BP6	500	12	492	493
BP7	1000	12	992	993

Table: The values of m_H , m_A and $\tan\beta$ chosen to probe the radiative return channel. The values of \sqrt{s} are also shown.

Benchmark	\mathcal{N}_S^{500}	\mathcal{N}_B^{500}	\mathcal{N}_S^{1000}	\mathcal{N}_B^{1000}	CL_{500}	CL_{1000}
BP6	1067.83	16110.05	2135.65	32220.08	8.14	11.12
BP7	146.55	1264.28	293.10	2528.57	3.90	5.51

Table: Number of signal and background surviving events in the radiative return process at the muon collider. Here $\mathcal{N}_S^{500(1000)}$ and $\mathcal{N}_B^{500(1000)}$ respectively denote the number of signal and background events at $\mathcal{L} = 500(1000) \text{ fb}^{-1}$. Besides, $CL_{500(1000)}$ denotes the confidence level at $\mathcal{L} = 500(1000) \text{ fb}^{-1}$.

Results: $50 \text{ GeV} < M_H < 90 \text{ GeV}$

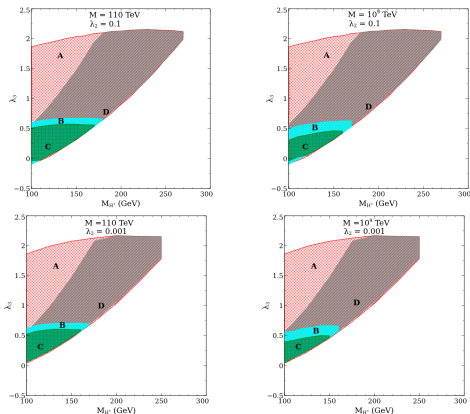


Figure: Regions allowed by the theoretical constraints projected in the $\lambda_3 - M_H^+$ plane for two values of λ_2 . The regions denoted by A (red), B (cyan) and C (green) obey those constraints up to $\Lambda_{UV} = 10^6$, 10^{16} and 10^{19} GeV respectively. The grey region denoted by D shows the 2σ allowed limit of the Higgs to diphoton signal strength.

Model: Type II 2HDM

- Fermions must couple to any one of the doublets in order to suppress FCNCs at the tree level. This can be achieved by invoking a \mathbb{Z}_2 symmetry.
- For the \mathbb{Z}_2 charge assignment $\Phi_1 \rightarrow -\Phi_1$ and $\psi_R^i \rightarrow -\psi_R^i$ (where ψ is a charged lepton or a down type quark), down-type quarks and leptons couple to Φ_1 . Up-type quarks couple to Φ_2 . (Type-II 2HDM).
- The Analytic forms of the 2HDM beta functions depend on the 2HDM "Type".
- We illustrate our findings in context of a Type II 2HDM.

S_3 HDM: Yukawa sector

- The Yukawa sector has yet more parameters! The RG analysis would turn unweildy. Must opt for some simplification. The 3rd generation of u-quarks is a singlet of S_3 .

$$\begin{aligned} -\mathcal{L}_Y &= y_1^u \left(\bar{Q}_1 \tilde{\phi}_3 u_{1R} + \bar{Q}_2 \tilde{\phi}_3 u_{2R} \right) \\ &+ y_2^u \left\{ \left(\bar{Q}_1 \tilde{\phi}_2 + \bar{Q}_2 \tilde{\phi}_1 \right) u_{1R} + \left(\bar{Q}_1 \tilde{\phi}_1 + \bar{Q}_2 \tilde{\phi}_2 \right) u_{2R} \right\} \\ &+ y_3^u \bar{Q}_3 \tilde{\phi}_3 u_{3R} + y_4^u \bar{Q}_3 \left(\tilde{\phi}_1 u_{1R} + \tilde{\phi}_2 u_{2R} \right) + y_5^u \left(\bar{Q}_1 \tilde{\phi}_1 + \bar{Q}_2 \tilde{\phi}_2 \right) u_{3R} + \text{h.c.} \end{aligned}$$

- Can explain the quark sector mass hierarchy, flavor mixing V_{CKM} and measure of CP violation naturally. (see [Teshima 2005](#))

Results: *active case.*

- Upper bound on $\tan\beta$ and $\lambda_i \rightarrow$ Tight scalar spectrum.

$$\text{Also, } \lambda_{h-H_i^+-H_i^-} \sim -\left(1 + \frac{m_h^2}{2m_{H_i^+}^2}\right) \rightarrow \mu_{\gamma\gamma} < 1.$$

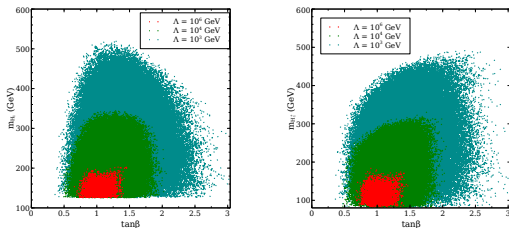


Figure: Bounds on the masses of H_1 and H_1^+ for different values of Λ .

- For $\Lambda = 10^6$ GeV, all non-standard masses < 300 GeV. An artifact of S_3 invariance and the chosen VEV alignment.

Main results: Inert scenario

Benchmark	m_{H_1} (GeV)	m_{A_1} (GeV)	$m_{H_1^+}$ (GeV)	λ_L	Ωh^2
BP3	57.00	102.00	120.00	0.0042	0.1170
BP7	718.600	727.450	727.225	0.0268	0.1263

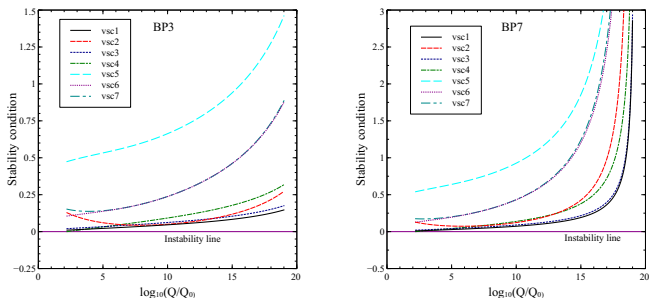


Figure: Evolution of the stability conditions for two benchmarks. The left and the right panel plots correspond to benchmarks from the $m_{H_1} < 80$ GeV and $m_{H_1} > 370$ GeV mass regions respectively. $M_t = 173$ GeV.

S_3 HDM beta functions

$$16\pi^2 \frac{dg_s}{dt} = -7g_s^3,$$

$$16\pi^2 \frac{dg}{dt} = -\frac{17}{6}g^3,$$

$$16\pi^2 \frac{dg'}{dt} = \frac{43}{6}g'^3.$$

$$16\pi^2 \beta_{\lambda_1} = 32\lambda_1^2 + 8\lambda_2^2 + 16\lambda_3^2 + 4\lambda_4^2 + 2\lambda_5^2 + \frac{1}{2}\lambda_6^2 - 8\lambda_1\lambda_2 + 16\lambda_1\lambda_3 \\ + 2\lambda_5\lambda_6 + 2\lambda_7^2 + \frac{3}{8}(g'^4 + 3g^4) - \lambda_1(9g^2 + 3g'^2)$$

$$16\pi^2 \beta_{\lambda_2} = 24\lambda_1\lambda_2 - 24\lambda_2^2 - 16\lambda_2\lambda_3 - \frac{1}{2}\lambda_6^2 + 2\lambda_7^2 - \frac{3}{4}g'^2g^2 \\ - \lambda_2(9g^2 + 3g'^2)$$

$$16\pi^2 \beta_{\lambda_3} = 16\lambda_3^2 + 8\lambda_4^2 + 24\lambda_1\lambda_3 + 8\lambda_2\lambda_3 + 8\lambda_4^2 + \frac{1}{2}\lambda_6^2 + 2\lambda_7^2 + \frac{3}{4}g'^2g^2 \\ - \lambda_3(9g^2 + 3g'^2)$$

Unitarity eigenvalues.

$$a^\pm = \left(\lambda_1 - \lambda_2 + \frac{\lambda_5 + \lambda_6}{2} \right) \pm \sqrt{\left(\lambda_1 - \lambda_2 + \frac{\lambda_5 + \lambda_6}{2} \right)^2 - 4 \left\{ (\lambda_1 - \lambda_2) \left(\frac{\lambda_5 + \lambda_6}{2} \right) - \lambda_4^2 \right\}},$$

$$b^\pm = (\lambda_1 + \lambda_2 + 2\lambda_3 + \lambda_8) \pm \sqrt{(\lambda_1 + \lambda_2 + 2\lambda_3 + \lambda_8)^2 - 4 \{ \lambda_8(\lambda_1 + \lambda_2 + 2\lambda_3) - 2\lambda_7^2 \}},$$

$$c^\pm = (\lambda_1 - \lambda_2 + 2\lambda_3 + \lambda_8) \pm \sqrt{(\lambda_1 - \lambda_2 + 2\lambda_3 + \lambda_8)^2 - 4 \left\{ \lambda_8(\lambda_1 - \lambda_2 + 2\lambda_3) - \frac{\lambda_6^2}{2} \right\}},$$

$$d^\pm = \left(\lambda_1 + \lambda_2 + \frac{\lambda_5}{2} + \lambda_7 \right) \pm \sqrt{\left(\lambda_1 + \lambda_2 + \frac{\lambda_5}{2} + \lambda_7 \right)^2 - 4 \left\{ (\lambda_1 + \lambda_2) \left(\frac{\lambda_5}{2} + \lambda_7 \right) - \lambda_4^2 \right\}},$$

$$e^\pm = (5\lambda_1 - \lambda_2 + 2\lambda_3 + 3\lambda_8) \pm \sqrt{(5\lambda_1 - \lambda_2 + 2\lambda_3 + 3\lambda_8)^2 - 4 \left\{ 3\lambda_8(5\lambda_1 - \lambda_2 + 2\lambda_3) - \frac{1}{2}(2\lambda_5 + \lambda_6)^2 \right\}},$$

$$f^\pm = \left(\lambda_1 + \lambda_2 + 4\lambda_3 + \frac{\lambda_5}{2} + \lambda_6 + 3\lambda_7 \right) \pm \sqrt{\left(\lambda_1 + \lambda_2 + 4\lambda_3 + \frac{\lambda_5}{2} + \lambda_6 + 3\lambda_7 \right)^2 - 4 \left\{ (\lambda_1 + \lambda_2 + 4\lambda_3) \left(\frac{\lambda_5}{2} + \lambda_6 + 3\lambda_7 \right) - 9\lambda_4^2 \right\}}$$

$$h_1 = \lambda_5 + 2\lambda_6 - 6\lambda_7,$$

$$h_2 = \lambda_5 - 2\lambda_7,$$

$$h_3 = 2(\lambda_1 - 5\lambda_2 - 2\lambda_3),$$

$$h_4 = 2(\lambda_1 - \lambda_2 - 2\lambda_3),$$

$$h_5 = 2(\lambda_1 + \lambda_2 - 2\lambda_3),$$

$$h_6 = \lambda_5 - \lambda_6.$$

Oblique parameters.

The expressions for the oblique parameters in the S_3 HDM are given. A shorthand notation $\sin(\beta - \alpha) = s_{\beta-\alpha}$, $\cos(\beta - \alpha) = c_{\beta-\alpha}$ is adopted,

$$\begin{aligned} \Delta S &= (2s_W^2 - 1)^2 G(m_{H_1^+}^2, m_{H_1^+}^2, m_Z^2) + (2s_W^2 - 1)^2 G(m_{H_2^+}^2, m_{H_2^+}^2, m_Z^2) + G(m_{H_2}^2, m_{A_1}^2, m_Z^2) \\ &\quad + c_{\beta-\alpha}^2 G(m_h^2, m_{A_2}^2, m_Z^2) + s_{\beta-\alpha}^2 G(m_{H_1}^2, m_{A_2}^2, m_Z^2) + c_{\beta-\alpha}^2 G(m_{H_1}^2, m_{H_1}^2, m_Z^2) \\ &\quad - s_{\beta-\alpha}^2 G(m_h^2, m_h^2, m_Z^2) - 2\ln(m_{H_1^+}^2) - 2\ln(m_{H_2^+}^2) + \ln(m_{H_2}^2) + \ln(m_{H_1}^2) + \ln(m_{A_1}^2) \\ &\quad + \ln(m_{A_2}^2) \end{aligned} \quad (\text{B.1a})$$

$$\begin{aligned} \Delta T &= F(m_{H_1^+}^2, m_{H_2}^2) + F(m_{H_1^+}^2, m_{A_1}^2) + c_{\beta-\alpha}^2 F(m_{H_2^+}^2, m_h^2) + s_{\beta-\alpha}^2 F(m_{H_2^+}^2, m_{H_1}^2) - F(m_{H_2}^2, m_{A_1}^2) \\ &\quad - c_{\beta-\alpha}^2 F(m_h^2, m_{A_2}^2) - s_{\beta-\alpha}^2 F(m_{H_1}^2, m_{A_2}^2) + 3c_{\beta-\alpha}^2 (F(m_Z^2, m_{H_1}^2) - F(m_W^2, m_{H_1}^2)) \\ &\quad - 3c_{\beta-\alpha}^2 (F(m_Z^2, m_h^2) - F(m_W^2, m_h^2)) \end{aligned} \quad (\text{B.1b})$$

$$\begin{aligned} \Delta U &= \frac{1}{24\pi} [G(m_{H_1^+}^2, m_{H_2}^2, m_W^2) + G(m_{H_1^+}^2, m_{A_1}^2, m_W^2) + c_{\beta-\alpha}^2 G(m_{H_2^+}^2, m_h^2, m_W^2) \\ &\quad + s_{\beta-\alpha}^2 G(m_{H_2^+}^2, m_{H_1}^2, m_W^2) + G(m_{H_2^+}^2, m_{A_2}^2, m_W^2) + c_{\beta-\alpha}^2 \hat{G}(m_{H_1}^2, m_W^2) - \hat{G}(m_{H_1}^2, m_Z^2) \\ &\quad - c_{\beta-\alpha}^2 \hat{G}(m_h^2, m_W^2) - \hat{G}(m_h^2, m_Z^2) - G(m_{H_2}^2, m_{A_1}^2, m_Z^2) - c_{\beta-\alpha}^2 G(m_h^2, m_{A_2}^2, m_Z^2) \\ &\quad - s_{\beta-\alpha}^2 G(m_{H_1}^2, m_{A_2}^2, m_Z^2) - (2s_W^2 - 1)^2 G(m_{H_1^+}^2, m_{H_1^+}^2, m_Z^2) \\ &\quad - (2s_W^2 - 1)^2 G(m_{H_2^+}^2, m_{H_2^+}^2, m_Z^2)] \end{aligned} \quad (\text{B.1c})$$

Oblique parameters.

where,

$$F(m_1^2, m_2^2) \equiv \begin{cases} \frac{m_1^2 + m_2^2}{2} - \frac{m_1^2 m_2^2}{m_1^2 - m_2^2} \ln \frac{m_1^2}{m_2^2} & ; m_1^2 \neq m_2^2, \\ 0 & ; m_1^2 = m_2^2. \end{cases}$$

$$G(m_1^2, m_2^2, q^2) \equiv -\frac{16}{3} + \frac{5(m_1^2 + m_2^2)}{q^2} - \frac{2(m_1^2 - m_2^2)^2}{(q^2)^2} \\ + \frac{3}{q^2} \left[\frac{m_1^4 + m_2^4}{m_1^2 - m_2^2} - \frac{m_1^4 - m_2^4}{q^2} + \frac{(m_1^2 - m_2^2)^3}{3q^4} \right] \ln \frac{m_1^2}{m_2^2} + \frac{r}{(q^2)^3} f(t, r)$$

$$\tilde{G}(m_1^2, m_2^2, q^2) \equiv -2 + \left(\frac{m_1^2 - m_2^2}{q^2} - \frac{m_1^2 + m_2^2}{m_1^2 - m_2^2} \right) \ln \frac{m_1^2}{m_2^2} + \frac{f(t, r)}{q^2}.$$

$$\hat{G}(m^2, q^2) \equiv G(m^2, m^2, q^2) + 12 \tilde{G}(m^2, m^2, q^2)$$

$$t \equiv m_1^2 + m_2^2 - q^2 \quad \text{and} \quad r \equiv (q^2)^2 - 2q^2(m_1^2 + m_2^2) + (m_1^2 - m_2^2)^2$$

$$f(t, r) \equiv \begin{cases} \sqrt{r} \ln \left| \frac{t - \sqrt{r}}{t + \sqrt{r}} \right| & ; r > 0, \\ 0 & ; r = 0, \\ 2\sqrt{-r} \tan^{-1} \frac{\sqrt{-r}}{t} & ; r < 0. \end{cases}$$